

Critical-field anisotropy and fluctuation conductivity in granular aluminum films

G. Deutscher* and S. A. Dodds

Department of Physics, University of California, Los Angeles, California 90024

(Received 12 November 1976)

We have measured the upper critical field $H_{c2}(\theta)$ for extreme type-II granular aluminum films much thicker than the coherence length and have found them to display a strong temperature-dependent anisotropy ($H_{\parallel}/H_{\perp} \gg 1$). The temperature dependence of the parallel critical field, $H_{\parallel}(T)$, shows an infinite slope near T_c , which we interpret as an indication that these films have a layered structure. The perpendicular critical field, $H_{\perp}(T)$, has an upward curvature, reminiscent of the behavior observed in $(\text{SN})_x$ and some layered compounds. As a result, the anisotropy ratio decreases strongly as the temperature is lowered. We interpret this behavior as a transition towards zero dimensionality (decoupled grains). We have also measured the fluctuation conductivity σ_s above T_c . We find that, for films with high values of normal-state resistivity, σ_s follows a power law characteristic of zero dimensionality far above T_c , and characteristic of two dimensionality closer to T_c , in agreement with the proposed interpretation of the critical-field data.

I. INTRODUCTION

It is well known that certain superconductors (e.g., aluminum) can be prepared in the form of granular films by evaporation in the presence of oxygen or coevaporation (or cosputtering) with an insulator.^{1,2} It is believed that in such films the metallic grains are separated by insulating barriers, which result in a high normal-state resistivity, ρ_n . Films with ρ_n values up to about $10^{-2} \Omega \text{ cm}$ are usually found to have a well-defined superconducting transition.^{2,3} As expected, high- ρ_n films behave like extreme type-II superconductors with critical fields much higher than the thermodynamic critical field of the bulk superconductor.^{4,5} Abeles *et al.*¹ and Cohen and Abeles⁴ reported measurements of $H_{\parallel}(T)$ and $H_{\perp}(T)$ for films with thicknesses in the range $300 < d < 900 \text{ \AA}$, and ρ_n values up to $10^{-3} \Omega \text{ cm}$. They concluded that the critical-field anisotropy ratio $H_{\parallel}(T)/H_{\perp}(T)$ essentially follows the Saint-James-de Gennes theory⁶ for the critical field of type-II films and that the absolute field values are in agreement with a theory for granular superconductors developed by Parmenter.⁷ In this theory the relevant coherence length that determines $H_{c2}(T)$ is calculated as a function of the transmission coefficient of the intergrain barriers, itself proportional to ρ_n . Hauser⁵ reached similar conclusions but reported critical-field values lower than predicted by the theory for $\rho_n \geq 10^{-3} \Omega \text{ cm}$. He ascribed this behavior to the presence of gross inhomogeneities in these films. Pettit and Silcox⁸ also reported some measurements of $H_{\perp}(T)$ similar to those of Refs. 1 and 4.

We present in this paper the results of critical-field measurements on aluminum films evaporated in the presence of oxygen with ρ_n values up to

several $10^{-2} \Omega \text{ cm}$ and thicknesses to several thousand \AA (typically 3000 \AA). The coherence length $\xi(T)$, is typically 10 to 100 times smaller than the thickness, so that the films should behave as bulk extreme type-II superconductors. We find, however, that this is not the case. The critical field is strongly anisotropic, with the parallel critical field, $H_{\parallel}(T)$, exhibiting negative curvature, and an infinite slope at T_c . The perpendicular field exhibits an unusual and quite pronounced upward curvature. We have also measured the fluctuation conductivity above T_c and find a behavior characteristic of a reduced dimensionality (two or zero) at temperatures $T \gg T_c$. This is in contrast to the usual behavior of thin films, which is three dimensional far from T_c [$d > \xi(T)$] and two dimensional close to T_c [$d < \xi(T)$].

Sample preparation and measuring techniques are detailed in Sec. II, and our results are presented in Sec. III. They are interpreted in Sec. IV in light of current theoretical models and experimental results for weakly coupled systems.

II. SAMPLE PREPARATION AND MEASUREMENT

Samples were prepared by evaporation of aluminum from an electron beam gun onto a quartz or glass substrate, mounted on a water-cooled holder. The pressure during the evaporation was held constant at approximately 5×10^{-5} Torr by admitting oxygen through a needle valve. Film composition was varied by controlling the deposition rate in the range $2\text{--}10 \text{ \AA}/\text{sec}$. After making the films, the oxygen supply was shut off, and four copper contact pads, about 1500 \AA thick, were evaporated over the films. Thicknesses were determined by a quartz crystal oscillator during deposition and

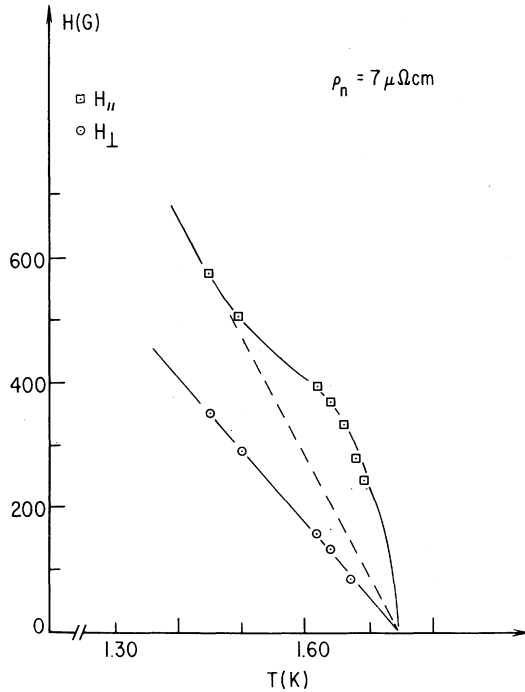


FIG. 1. Temperature dependence of the critical field for a slightly dirty film. Curves are shown for fields applied parallel, $H_{||}$, or perpendicular, H_{\perp} , to the film surface. Normal-state resistivity, measured at 4.2 K with a field of 15 kG applied in the perpendicular direction, is indicated in each figure.

verified with an optical interferometer after removal from the vacuum system.

Resistance measurements were carried out by the conventional dc four-probe technique, using pressure contacts onto the evaporated copper pads. The maximum measuring current used was 1 mA, and much smaller currents were used for the high resistivity films. Samples were immersed in liquid helium during the measurements, and the temperature was determined by measuring the vapor pressure over the bath. A magnetic field was provided by an iron core electromagnet controlled by a Varian Fieldial. The magnet could be rotated to align the field either parallel or perpendicular to the film surface. The applied field was always perpendicular to the measuring current.

The critical temperature, T_c , was defined as the temperature at which the resistivity reached half its normal-state value. The critical fields were defined by the same criterion. In both cases, the normal-state resistivity was taken to be the value measured with a field of 15 kG applied perpendicular to the sample, at a temperature of 4.2 K.

As a partial check on the gross homogeneity of the material, the microwave frequency (9.2 GHz) resistivity of several of the samples was measured as a function of temperature and field. For these measurements, the critical fields and temperatures were defined as the values at which half the total change in reflected microwave voltage occurred. Although the definition of T_c and H_c is somewhat arbitrary for both the dc and microwave measurements, the same qualitative behavior was seen in both. As an example, we shall show in Fig. 6 the dependence of H_c on magnetic field angle, as determined by both microwave and dc measurements. The same angular dependence is clearly seen by both methods. Since the penetration depth in these very dirty films is much greater than the sample thickness,⁵ the agreement of the two methods gives us some confidence that we are observing an essentially bulk property of the sample.

III. RESULTS

In this section, we present our results for the critical fields $H_{||}(T)$ and $H_{\perp}(T)$, the angular dependence $H_{c2}(\theta)$ and the fluctuation conductivity above T_c . These results were obtained from a series of samples, all about 3000 Å thick, with ρ_n values ranging from a few 10^{-6} to a few 10^{-2} Ω cm.

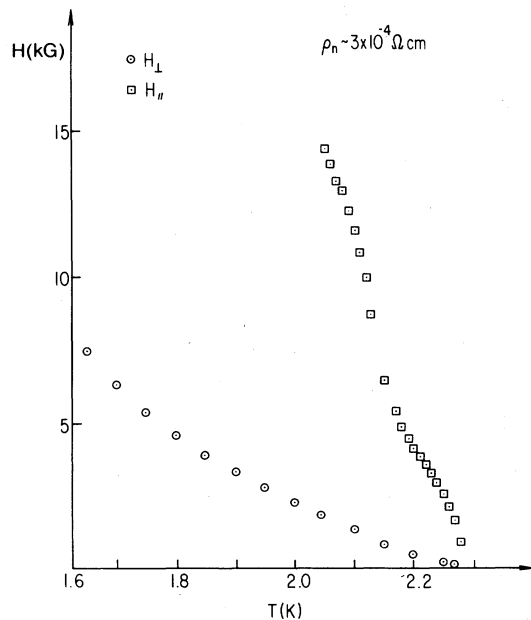


FIG. 2. Temperature dependence of the critical field for a moderately dirty film.

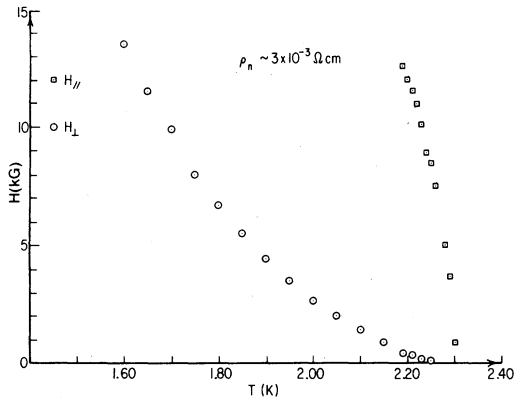


FIG. 3. Temperature dependence of the critical field for a very dirty film.

A. Parallel critical fields

The results for $H_{\parallel}(T)$ are shown in Figs. 1–5 in order of increasing ρ_n values. Figure 1 exhibits behavior typical of a slightly dirty ($\rho_n \approx 10^{-5} \Omega \text{ cm}$) Al film. It is just the characteristic behavior of a type-II film with $d < \xi(T)$ near T_c , giving rise to the infinite slope at T_c , and $d > \xi(T)$ at low temperatures, where $H = H_{c3} = 1.7 H_{c2}$.^{6,9} Figure 2 exhibits critical-field data for a moderately dirty film ($\rho_n \approx 3 \times 10^{-4} \Omega \text{ cm}$). The magnitude of H_{\parallel} has increased considerably. The slope at T_c is still infinite, but somewhat below T_c , $H_{\parallel}(T)$ shows a very clear upturn. To our knowledge, such behavior has never been reported before. As in Fig. 1, the behavior very near T_c may be understood by assuming that the condition

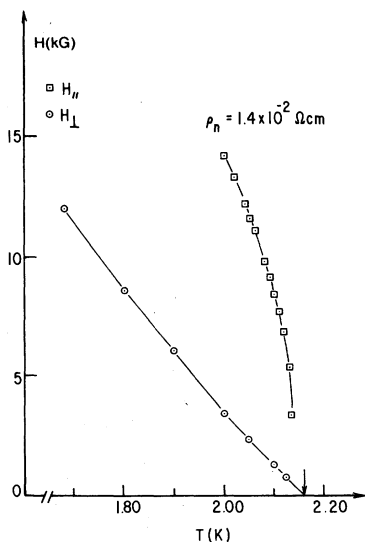


FIG. 4. Temperature dependence of the critical field for a very dirty film.

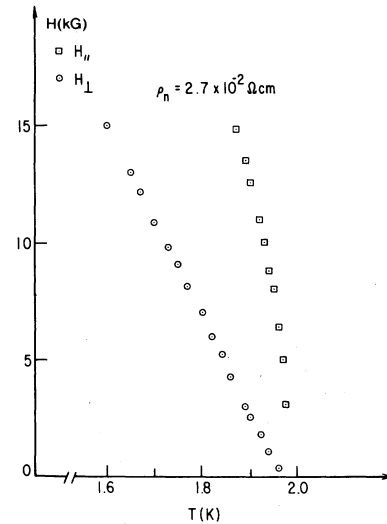


FIG. 5. Temperature dependence of the critical field for a very dirty film.

$d < \xi(T)$ is still fulfilled for that sample but now in a narrower temperature range near T_c . The upward curvature observed around $T = 2.15 \text{ K}$ can certainly not be understood on the basis of the theory for a homogeneous type-II film.

Results shown in Figs. 3–5 are for very dirty films ($\rho_n > 10^{-3} \Omega \text{ cm}$). $H_{\parallel}(T)$ still has a parabolic form, which is quite surprising in view of the fact that the coherence length $\xi(T=0)$ in such films should be^{1,4,7} one to two orders of magnitude smaller than the thickness. The condition $\xi(T) > d$ should only hold within a few tens of millidegrees of T_c , resulting in an essentially linear behavior of $H_{\parallel}(T)$. These samples are actually behaving as very thin films with $d \ll \xi(T)$, although they are in fact very thick. This behavior is suggestive of a “layered” structure. An additional surprising feature is that the magnitude of $H(T)$ is essentially the same for these three films, although ρ_n varies amongst them by an order of magnitude.

B. Perpendicular critical fields

Referring again to Figs. 1–5, we follow the same order as in Sec. IIIA. The slightly dirty films behave as regular type-II films, with $H_{\perp}(T)$ varying linearly as a function of temperature (Fig. 1). In moderately dirty films (Fig. 2), there is a slight indication of an upward curvature, especially at the lower temperatures. This upward curvature is very clear in Fig. 3, where it exists in the whole temperature range covered in the experiment. Unlike what happens in the parallel orientation, the magnitude of H_{\perp} continues to increase when ρ_n increases beyond $10^{-3} \Omega \text{ cm}$, as

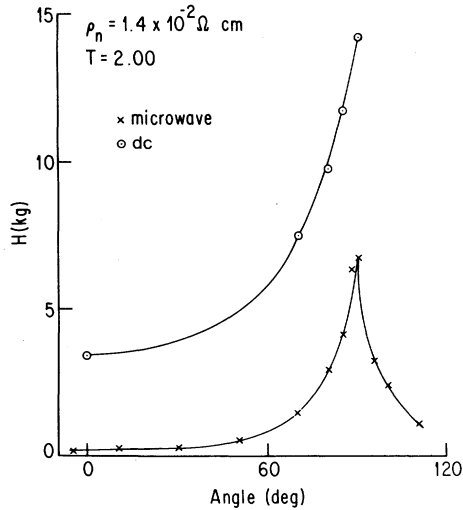


FIG. 6. Critical field as a function of the angle between the applied field and the normal to the film surface for the same sample as in Fig. 4. Note that the angular dependence of the microwave (9.2 GHz) measurements is the same as that of the dc measurements.

can be seen in Figs. 4 and 5. The upward curvature is still present, but now becomes more localized near T_c as ρ_n is increased.

Although the reason for the upward curvature in $H_{\perp}(T)$ is not obvious, we can make two remarks: first, the same sort of model should be able to explain the upward curvature observed in $H_{\parallel}(T)$ for $\rho_n \approx 10^{-4} \Omega \text{ cm}$ and in $H_{\perp}(T)$ for $\rho_n > 10^{-3} \Omega \text{ cm}$; second, this model should explain the general

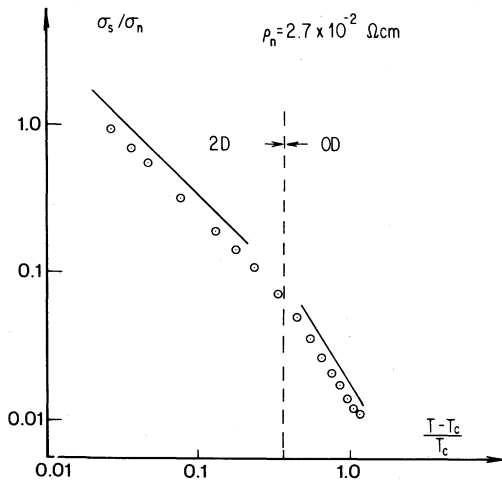


FIG. 7. Temperature dependence of the excess conductivity above T_c , for the same sample as in Fig. 5. As noted in the text, T_c is taken to be the temperature at which the resistance falls to half its normal state value. Solid lines indicate the slopes expected in various dimensionality regimes.

pattern displayed by these results: namely, that the region of upward curvature in $H_{\perp}(T)$ moves from low temperatures to high temperatures as ρ_n is increased. Upward curvature of critical fields has previously been observed in layered compounds¹⁰ and in the polymeric superconductor $(\text{SN})_x$.¹¹

C. Angular dependence $H_{c2}(\theta)$

The angular dependence of the upper critical field is always of the form shown in Fig. 6, with a marked cusp at the parallel orientation. Both the parabolic form of $H_{\parallel}(T)$ and the large values of the anisotropy ratio suggest the presence of a layered structure. This form of the angular dependence is of interest because it shows that the films cannot in general be described by an effective mass theory.¹² Such a theory predicts a zero slope for $H_{c2}(\theta)$ around the parallel orientation, and a temperature-independent anisotropy ratio, both of which are contrary to our observations.

D. Fluctuation conductivity

For the extremely dirty films, Fig. 7, the fluctuation conductivity indicates that $\sigma_s/\sigma_n \propto (T - T_c/T_c)^2$ far above T_c . This behavior is characteristic of zero dimensionality,¹³ and in fact has been observed previously by Kirtley *et al.*¹⁴ in very weakly coupled Sn powders. Closer to T_c , $\sigma_s/\sigma_n \propto (T - T_c/T_c)^{-1}$, a behavior characteristic of two dimensionality. There is no evidence of a three-dimensional regime in the immediate vicinity of T_c .

The behavior of moderately dirty films, Fig. 8,

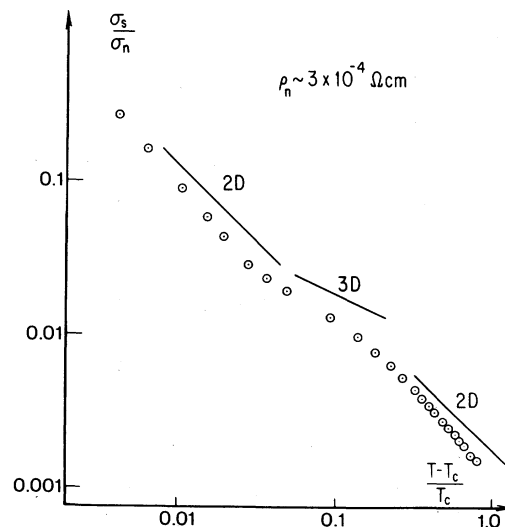


FIG. 8. Temperature dependence of the excess conductivity above T_c , for the same sample as in Fig. 2.

is quite different. There one observes a two-dimensional behavior far above T_c , followed by an "aborted" transition towards three dimensionality, with the behavior close to T_c tending to two dimensional again.

These results should be treated with some caution because: (a) close to T_c the behavior depends very much on the choice that one makes for T_c ; and (b) far from T_c the value taken for σ_n has a strong influence on the shape of $\sigma_s(T)$. As explained in Sec. I, σ_n was taken to be the value of σ at 4.2 K when a perpendicular field of 15 kG was applied. This field may not have been sufficient to completely quench superconducting fluctuations in the dirtiest films. However, a slightly different value for σ_n would not greatly affect the behavior shown in Fig. 7, simply because σ_s is already quite large for such dirty films at 4.2 K. Still, measurements of σ_n using higher fields are clearly desirable.

IV. INTERPRETATION AND DISCUSSION

The most prominent feature of the data is the anisotropy of the critical field. In thin films such an anisotropy may in principle be due to two different mechanisms.

(a) For films thinner than the coherence length $\xi(T)$, the parallel critical field is given by

$$H_{\parallel} = \sqrt{12} [\phi_0/2\pi d\xi(T)], \quad (1)$$

while the perpendicular critical field is

$$H_{\perp} = \phi_0/2\pi\xi^2(T) \quad (2)$$

giving an anisotropy ratio

$$H_{\parallel}/H_{\perp} = \sqrt{12} [\xi(T)/d], \quad (3)$$

where d is the film thickness and ϕ_0 is the flux quantum. These expressions fit the data for relatively clean films rather well (Fig. 1). Calculating $\xi(T)$ from Eq. (2), one obtains a value larger than the thickness in the temperature range near T_c , where $H_{\parallel}(T)$ shows a parabolic behavior in accordance with Eq. (1). The anisotropy ratio is constant at lower temperatures and equal to 1.7, as it should be in the surface superconductivity regime^{6,9} where $d \geq 2\xi(T)$.

(b) Another interpretation must be given for the dirtier samples (Figs. 3–5). There, if one calculates $\xi(T)$ from Eq. (2), one finds that it is larger than d only within about 10 mK of T_c , while a large anisotropy is still observed at lower temperatures. On the basis of $\xi(T)$, then, these films are essentially bulk superconductors. The critical-field anisotropy must therefore reflect some internal anisotropic structure in the films. Defining $\xi_{\parallel}(T)$ and $\xi_{\perp}(T)$ as the coherence lengths,

respectively, in the directions parallel and perpendicular to the surface of the films, the critical fields in the effective-mass approximation are given by¹²

$$H_{\parallel}(T) = \phi_0/2\pi\xi_{\parallel}(T)\xi_{\perp}(T), \quad (4)$$

$$H_{\perp}(T) = \phi_0/2\pi\xi_{\parallel}^2(T), \quad (5)$$

$$H_{\parallel}/H_{\perp} = \xi_{\parallel}(T)/\xi_{\perp}(T). \quad (6)$$

Although these expressions predict a temperature-independent anisotropy ratio, contrary to what is observed in the experiments, we must retain the general idea that $\xi_{\parallel}(T) > \xi_{\perp}(T)$. Since the short coherence length in these films is known to be due to the presence of oxide between the grains, we conclude that there is more oxide between superimposed grains than between collateral grains. In other words, these films have a sort of layered structure.

The temperature dependence of $H_{\parallel}(T)$ shows essentially a parabolic variation for the dirtier samples (Figs. 3–5) in the range of temperatures where it could be measured, and can be explained in two ways. It may be that superimposed layers of grains are essentially decoupled, in which case $H_{\parallel}(T)$ would be given by Eq. (1) with d equal to the thickness of the layers. Alternatively, $H_{\parallel}(T)$ may be set by the paramagnetic limit. Although our data for $H_{\parallel}(T)$ are limited to the region near T_c , we find a magnitude and temperature dependence¹⁵ consistent with paramagnetic limit in the dirtiest samples. Also, we observe that $H_{\parallel}(T)$ hardly changes when ρ_n is increased from $3 \times 10^{-3} \Omega \text{ cm}$ to $2.7 \times 10^{-2} \Omega \text{ cm}$, while dH_{\perp}/dT continues to increase, again suggesting that the Pauli susceptibility limits $H_{\parallel}(T)$.

The question of whether superimposed layers of grains are effectively coupled or not can best be discussed by looking at the data for a moderately dirty film (Fig. 2). There we observe a very peculiar behavior of $H_{\parallel}(T)$, with a marked upward curvature for $T \approx 2.15$ K. Such behavior has been predicted to occur in layered compounds¹² when the layers are effectively coupled near T_c but decoupled at low temperature. The crossover between the coupled and the uncoupled regimes occurs at the temperature where $\sqrt{2}\xi_{\perp}(T)$ is equal to the separation between the layers. In our case the separation is the grain size d plus the oxide thickness s .¹⁶ We therefore use Eqs. (4) and (5) to calculate $\xi_{\perp}(T)$ at the crossover temperature T_c , taken as the inflection point of the $H(T)$ curve ($T_c \approx 2.12$, $H_{\perp} \approx 900$ G, $\xi_{\parallel}/\xi_{\perp} = H_{\parallel}/H_{\perp} \approx 8$). We obtain $\xi_{\perp}(T = T_c) \cong 70 \text{ \AA}$ and $d + s \cong 100 \text{ \AA}$, in fair agreement with measured grain sizes (30–40 \AA),³ and compositions (30–40% oxide²) of such films. We conclude that, in moderately dirty films,

superimposed layers of grains are effectively coupled over a sizable temperature range near T_c . In the dirtiest films, the coupling is practically ineffective at all temperatures, and $H_{||}(T)$ is probably set at all temperatures by the paramagnetic limit.

We now turn our attention to the behavior of $H_{\perp}(T)$. Its main feature is the existence of a region of upward curvature, starting at low temperatures for moderately dirty films (Fig. 2) and moving closer to T_c for dirtier films. By analogy to our interpretation of $H_{||}(T)$ (Fig. 2) we attribute this behavior to a progressive decoupling of the grains in the lateral directions. Generally speaking, as one makes the samples dirtier and goes towards lower temperatures, i.e., when one reduces $\xi(T)$, one first decouples superimposed layers of grains, which increases the anisotropy ratio, and then one tends to decouple the grains in all directions, which decreases the anisotropy. Eventually, for dirty enough samples and low enough temperatures, one should reach the zero-dimensional limit¹³ with an anisotropy ratio of order unity. By extrapolating the behavior shown in Figs. 4 and 5, one would expect the zero-dimensional limit to be reached for these samples around 1 K. A more quantitative interpretation of the critical-field data will have to wait until calculations are available for the case where the thickness of the superconducting grains (or layers) cannot be neglected, unlike the situation encountered in layered compounds.¹²

Finally, we wish to comment on the fluctuation conductivity measurements and relate them to the critical-field data. At temperatures far above T_c the behavior of the dirtiest samples (Fig. 7) is reminiscent of that observed for amorphous superconductors,¹⁷ but close to T_c there is a difference that we attribute to the layering of our films, which then show a two-dimensional rather than three-dimensional behavior. In cleaner samples (Fig. 8), the zero-dimensional regime is not reached up to $(T - T_c)/T_c \approx 1$. Although there seems to be evidence for a continuing curvature, the behavior is rather more two dimensional, again in agreement with the critical-field data. Below $t_{t+} = (T - T_{t+})/T_c \approx 0.15$, the behavior becomes three-dimensional (3D) like. From the critical-field data for the same sample (Fig. 2) we concluded that the 3D-2D crossover occurs at $t_{t-} = (T - T_{t-})/T_c \approx 0.06$. According to theory^{12,13} one expects $t_{t+}/t_{t-} = 2$, in fair agreement with the experiment. The behavior of σ_s very close to T_c is somewhat uncertain, depending on the choice that one makes for T_c , but there is some indication

that the behavior is again two dimensional, in agreement with the critical-field data. This seems to happen within about 20 mK of T_c , a temperature range where the coherence length may become of the order of the film thickness.

From the fluctuation conductivity data it would appear that in the dirtiest sample the 2D-0D dimensionality crossover occurs at $t_{t+} = 0.37$. One would therefore expect¹³ that $t_{t-} = 0.74$. In other words, below $T_{t-} = 0.5$ K there should be no anisotropy in the critical field. Although we do not have data in that temperature range, extrapolation of the available high-temperature data (Fig. 5) is certainly consistent with that assumption.

There is some difficulty with the estimation of the coherence length $\xi_{||}(T_{t-})$ at which 0D behavior is reached. First, we do not have critical-field data in that temperature range. Second, even if these data were available, it is likely that they would be dominated by the limiting effect of the Pauli susceptibility. Using the H_{\perp} data near T_c to estimate $\xi(T)$, one finds $\xi(T=0) \approx 60$ Å, slightly larger than the grain size. It is also possible to estimate $\xi(T)$ from the measured value of ρ_n .^{7,13} This gives $\xi(T=0) \approx 20$ Å, somewhat smaller than the grain size. In either case, a transition to 0D in such films for $t_t \leq 1$ is reasonable.

V. CONCLUSIONS

Granular aluminum films prepared by evaporation in the presence of oxygen have an anisotropic structure: superimposed layers of grains are separated by thicker oxide layers than collateral grains. By measuring the critical fields and fluctuation conductivity as a function of oxide content and temperature, we have been able to observe the 3D-2D crossover where superimposed layers of grains become decoupled, and the 2D-0D crossover where collateral grains become decoupled. Critical-field measurements, $H_{c2}(\theta)$, on films with $\rho_n > 10^{-3}$ Ω cm should provide a more complete picture of the latter crossover.

ACKNOWLEDGMENTS

We are much indebted to Raymond Orbach for frequent stimulating and enjoyable discussions during the course of this work. One of us (G. D.) would like to acknowledge the hospitality of Rutgers University, where part of the manuscript was written. This work was supported in part by the U. S. Office of Naval Research under Contract ONR-N00014-75-C-0245, and in part by the National Science Foundation under grants NSF DMR 75-19544 and NSF DMR 72-02935 A03.

- *Permanent address: Department of Physics, Tel Aviv University, Tel Aviv, Israel.
- ¹B. Abeles, R. W. Cohen, and W. R. Stowell, *Phys. Rev. Lett.* **18**, 902 (1967).
- ²B. Abeles and J. J. Hanak, *Phys. Lett. A* **34**, 165 (1971).
- ³G. Deutscher, M. Gershenson, E. Grunbaum, and Y. Imry, *J. Vac. Sci. Technol.* **10**, 697 (1973); G. Deutscher, H. Fenichel, M. Gershenson, E. Grunbaum, and Z. Ovadyahu, *J. Low Temp. Phys.* **10**, 231 (1973).
- ⁴R. W. Cohen and B. Abeles, *Phys. Rev.* **168**, 444 (1968).
- ⁵J. J. Hauser, *J. Low Temp. Phys.* **7**, 335 (1972).
- ⁶D. Saint-James and P. G. de Gennes, *Phys. Lett.* **7**, 306 (1963); however, the data shown in Fig. 3 of Ref. 4 show that H_{\parallel}/H_{\perp} is systematically somewhat higher than the theoretical value.
- ⁷R. H. Parmenter, *Phys. Rev.* **154**, 353 (1967).
- ⁸R. B. Pettit and J. Silcox, *Phys. Rev. B* **13**, 2865 (1976).
- ⁹J. P. Burger, G. Deutscher, E. Guyon, and A. Martin-
et, *Phys. Rev. A* **137**, 853 (1965).
- ¹⁰J. Wollam, R. Somoano, and P. O'Connor, *Phys. Rev. Lett.* **32**, 712 (1974).
- ¹¹L. J. Azevedo, W. G. Clark, G. Deutscher, R. L. Greene, G. B. Street, and L. J. Suter, *Solid State Commun.* **19**, 197 (1976).
- ¹²R. A. Klemm, A. Luther, and M. R. Beasley, *Phys. Rev. B* **12**, 877 (1975).
- ¹³G. Deutscher, Y. Imry, and L. Gunther, *Phys. Rev. B* **10**, 4598 (1974).
- ¹⁴J. Kirtley, Y. Imry, and P. Hansma, *J. Low Temp. Phys.* **17**, 247 (1974).
- ¹⁵K. Maki and T. Tsuneto, *Prog. Theor. Phys. (Kyoto)* **31**, 945 (1964).
- ¹⁶G. Deutscher and O. Entin-Wohlman (unpublished).
- ¹⁷W. L. Johnson and C. C. Tsuei, *Phys. Rev. B* **13**, 4827 (1976).